

*Short Note*

## **Cholesterol Dependent Uptake and Interaction of Doxorubicin in MCF-7 Breast Cancer Cells**

**Petra Weber, Michael Wagner and Herbert Schneckenburger \***

Institut für Angewandte Forschung, Hochschule Aalen, Anton-Huber Str. 21, 73430 Aalen, Germany;  
E-Mails: petra.weber@htw-aalen.de (P.W.); michael.wagner@htw-aalen.de (M.W.)

\* Author to whom correspondence should be addressed;  
E-Mail: herbert.schneckenburger@htw-aalen.de; Tel.: +49-7361-576-3401.

*Received: 25 February 2013; in revised form: 3 April 2013 / Accepted: 8 April 2013 /  
Published: 16 April 2013*

---

**Abstract:** Methods of fluorescence spectroscopy and microscopy—including intensity and lifetime (FLIM) images—are used to examine uptake, intracellular location and interaction of the chemotherapeutic drug doxorubicin in MCF-7 human breast cancer cells as a function of cholesterol content. By comparing cells with natural and decreased cholesterol levels after 2 h or 24 h incubation with doxorubicin, we observed that higher fluorescence intensities and possibly shortened fluorescence lifetimes—reflecting increased uptake of the drug and more pronounced drug response—are concomitant with higher membrane fluidity.

**Keywords:** cancer cells; doxorubicin; cholesterol; fluorescence lifetime imaging microscopy (FLIM)

---

### **1. Introduction**

Doxorubicin, an anthracycline antibiotic, is used as a cytostatic drug in cancer chemotherapy, such as breast cancer, bronchial carcinoma and lymphoma, and has been studied for several decades [1,2]. The drug is taken up by cells due to passive diffusion through their membrane and finally intercalates in DNA strands, where it causes chromatin condensation and initiates apoptosis [3]. Due to its fluorescence properties [4] doxorubicin can be localized within the cells, e.g., by wide-field microscopy, and, furthermore, fluorescence lifetime measurements [5–8] permit assessing

intermolecular interactions with its microenvironment. Low or moderate light doses are needed to avoid phototoxic effects in microscopic experiments [9].

In the last years various approaches for improvement of chemotherapy have been used, including encapsulation of chemotherapeutic drugs [10] or combination therapy with sensitizing substances for apoptosis [11]. If a free drug, e.g., doxorubicin, is applied, its cellular uptake may depend on membrane properties [12–15], in particular on cholesterol content which has been shown to have a high impact on membrane stiffness and fluidity [16,17]. To evaluate this impact, intracellular cholesterol was modified in the present paper with reference to a well known protocol [18]. Using this protocol, cholesterol content in U373-MG glioblastoma cells was previously reduced by about 50% upon application of 4 mM methyl- $\beta$ -cyclodextrin (M $\beta$ CD) [16]. “Untreated” and “cyclodextrin treated” cells will be distinguished further.

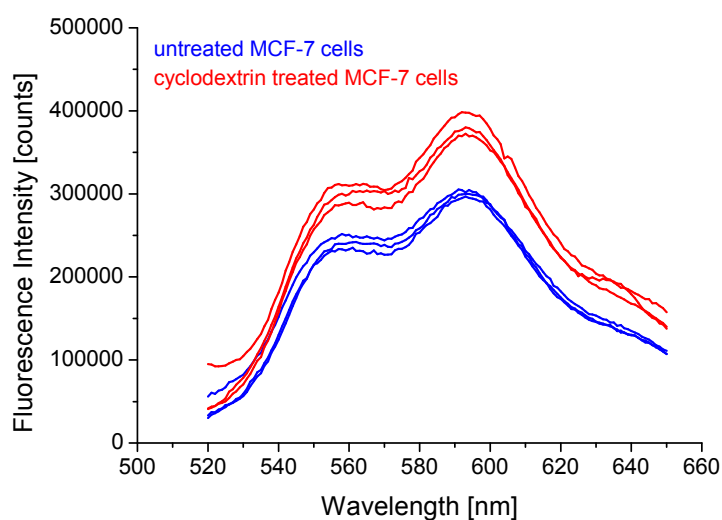
In the present manuscript fluorescence spectroscopy of suspensions of MCF-7 human breast cancer cells is combined with microscopic measurements of fluorescence images (including fluorescence lifetime images, FLIM) as well as fluorescence decay kinetics of MCF-7 cell monolayers located on an object slide. A low concentration and two different incubation times (2 and 24 h) of free doxorubicin (2  $\mu$ M) are chosen in order to examine early steps of apoptosis with (almost) unchanged cell morphology.

## 2. Results and Discussion

### 2.1. Intensity of Doxorubicin Fluorescence Increases after Cholesterol Depletion

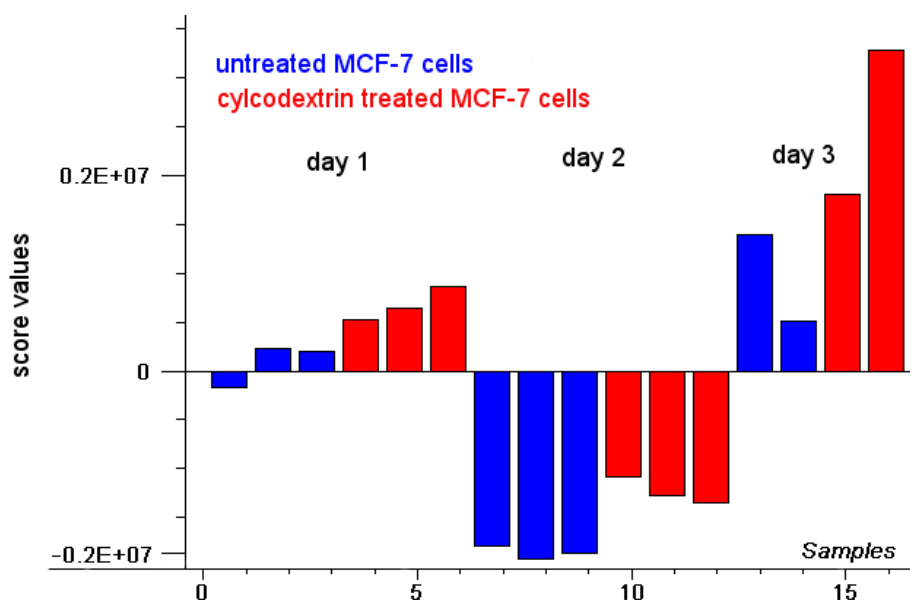
To examine cholesterol dependent cellular uptake of doxorubicin, we determined fluorescence intensity of untreated and cyclodextrin treated MCF-7 cells, after incubation with doxorubicin (2  $\mu$ M) for 24 h. Fluorescence spectra are depicted in Figure 1 for three independent measurements of cell suspensions ( $1 \times 10^6$  cells) in each case. Obviously, the untreated cells show lower fluorescence intensities than cells upon cholesterol depletion.

**Figure 1.** Fluorescence spectra of MCF-7 cells incubated with doxorubicin (2  $\mu$ M, 24 h); spectra of three suspensions of  $10^6$  cells each; untreated cells (lower curves) and cyclodextrin treated cells (upper curves) obtained during one series of experiments are compared; excitation wavelength:  $\lambda_{\text{ex}} = 470$  nm.



Two further series of experiments were performed with MCF-7 cells, and although fluorescence intensity generally varied between these series, it was always lower for untreated, in comparison with cyclodextrin treated cells. For a common evaluation of all fluorescence spectra, the method of principal component analysis (PCA), a multivariate statistical method [19,20] was used. This method reduces multi-dimensional data into a few principal components which constitute a new, lower dimensional coordinate system for describing the fluorescence spectra. Common information explaining as much of the spectral variation as possible is summarized in the principal components (PCs), each one being represented by a loading spectrum and score values describing the individual spectra in the new PC coordinate system. According to PCA, 98% of spectral information was given by fluorescence intensity (PC 1) with a loading plot representing the mean fluorescence spectrum. The scores depicted in Figure 2 quantify all individual fluorescence spectra related to PC1, *i.e.*, negative scores describe spectra of lower fluorescence intensity, whereas positive scores describe spectra of higher fluorescence intensity in comparison with the mean spectrum. Figure 2 proves that fluorescence intensities were different for the three series of experiments, but in each case the scores were either more positive or less negative for the cyclodextrin treated cells in comparison with the untreated controls, thus proving higher fluorescence intensity after cholesterol depletion. It is assumed that after cholesterol depletion cell membranes were more fluid, and that the uptake of doxorubicin was, therefore, enhanced.

**Figure 2.** Principal component analysis (PCA); scores plot of PC1 (fluorescence intensity) for a set of 16 individual spectra obtained from three series (3 days) of experiments with samples of untreated and cyclodextrin treated MCF-7 cells.

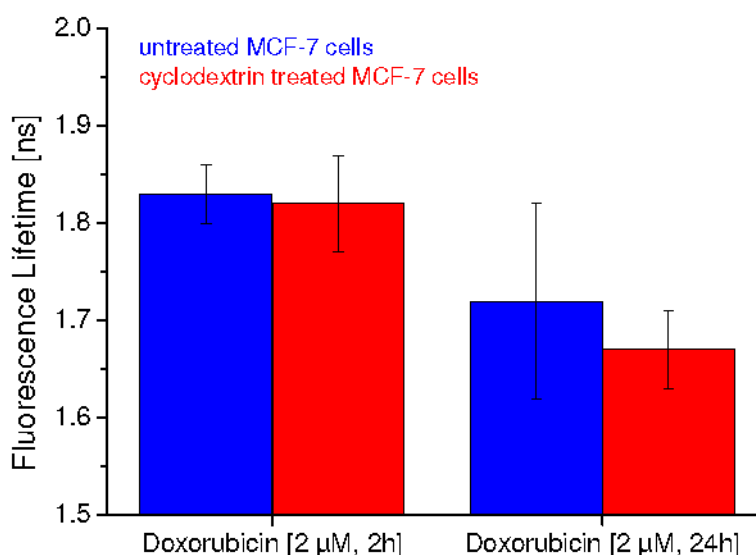


## 2.2. Fluorescence Lifetime Decreases as a Function of Doxorubicin Incubation Time and Cholesterol Content

Fluorescence lifetimes of MCF-7 breast cancer cells upon 2 h or 24 h incubation with doxorubicin (2  $\mu$ M) are depicted in Figure 3. While fluorescence lifetimes of untreated and cyclodextrin treated cells were almost the same ( $1.83 \pm 0.03$  ns and  $1.82 \pm 0.05$  ns, respectively) after 2 h incubation with

doxorubicin, they decreased to  $1.72 \pm 0.10$  ns for untreated and  $1.67 \pm 0.04$  ns for cyclodextrin treated cells after 24 h incubation. Decrease in fluorescence lifetime may result from apoptosis, as earlier reported for HeLa cells [5]. This decrease appeared to be more pronounced upon cholesterol depletion by M $\beta$ CD, possibly due to an increased uptake of doxorubicin and, consequently, a more rapid apoptotic process. A non-directional Mann-Whitney  $U$  test with a level of significance  $\alpha = 5\%$  proved that the decrease of fluorescence lifetimes between 2 and 24 h incubation was not significant for untreated cells, but significant for cyclodextrin treated cells. Also the difference of fluorescence lifetimes at 24 h incubation between untreated and cyclodextrin treated cells revealed to be non-significant; however a tendency towards shortened fluorescence lifetimes upon cyclodextrin treatment can be deduced from Figure 3.

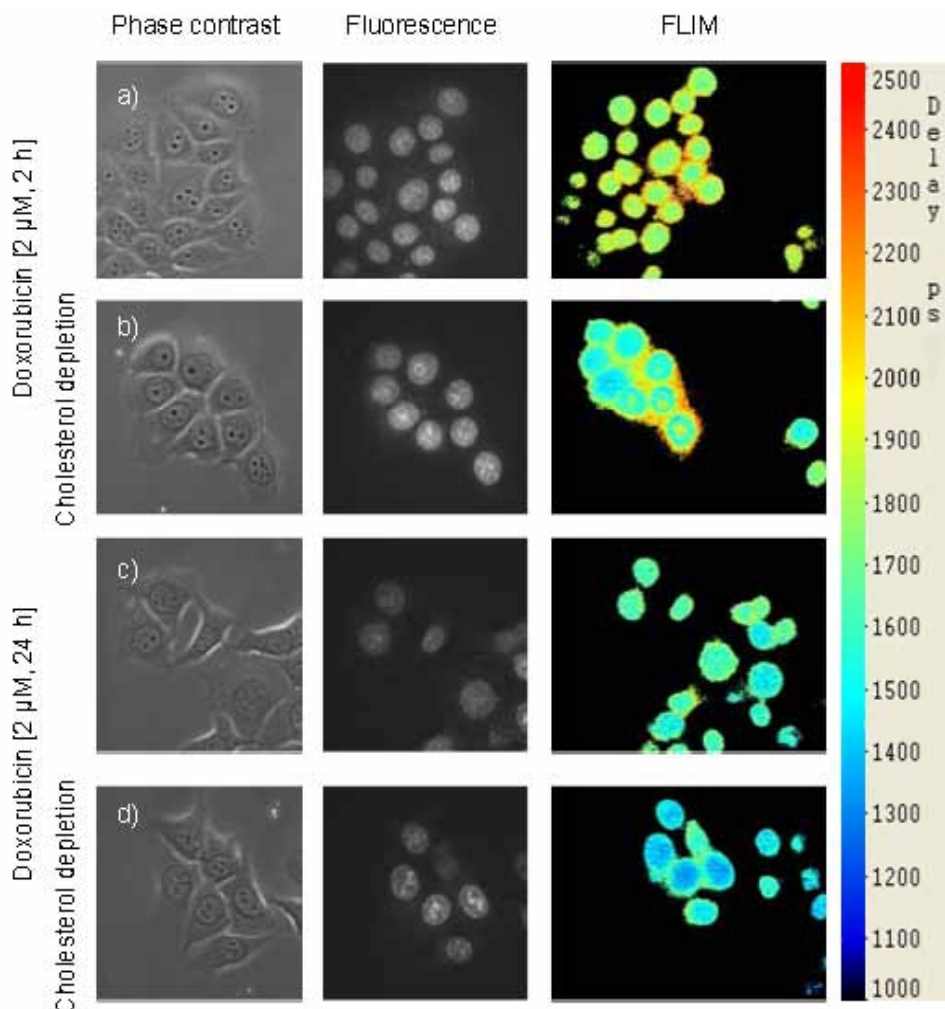
**Figure 3.** Fluorescence lifetime of untreated (blue bars) or cyclodextrin treated (red bars) MCF-7 cell monolayers after incubation with doxorubicin ( $2 \mu\text{M}$ ) for 2 h or 24 h, respectively. Excitation wavelength:  $\lambda_{\text{ex}} = 470$  nm; medians and median absolute deviations (MADs) of 15 measurements (untreated cells) or eight measurements (cyclodextrin treated cells) are indicated.



### 2.3. Images

In Figure 4 phase contrast, fluorescence intensity and fluorescence lifetime (FLIM) images of untreated and cyclodextrin treated MCF-7 cells incubated for 2 or 24 h with doxorubicin ( $2 \mu\text{M}$ ) are depicted. While fluorescence of doxorubicin is well located in the cell nucleus, its lifetime shows a similar behaviour as depicted in Figure 3 with a decrease in fluorescence lifetime after 24 h incubation, which was more pronounced in the case of reduced (after cyclodextrin treatment) than in the case of natural cholesterol content. This indicates possible changes of intermolecular interaction, e.g., upon DNA strand breaks [5] and proves the potential of FLIM measurements for detection of these changes in processes like apoptosis.

**Figure 4.** Phase contrast images, fluorescence intensities and effective fluorescence lifetimes  $\tau_{\text{eff}}$  in picoseconds (from left to right) of MCF-7 cells incubated with doxorubicin (2  $\mu\text{M}$ ) for 2 h (a,b) or 24 h (c,d); untreated cells (a,c) and cyclodextrin treated cells (b,d) are compared. Excitation wavelength:  $\lambda_{\text{ex}} = 470 \text{ nm}$ ; fluorescence recorded at  $\lambda \geq 520 \text{ nm}$ ; image size:  $140 \mu\text{m} \times 140 \mu\text{m}$  each.



The observed decrease of fluorescence lifetime of intracellular doxorubicin as a function of the incubation time is in agreement with the literature and indicates beginning apoptosis [5–7]. In addition, we could show that the uptake of doxorubicin is enhanced and that the process of apoptosis may be accelerated, if membrane fluidity is increased upon cholesterol depletion. This indicates that biophysical properties may have some impact on the uptake and the efficiency of chemotherapeutic drugs. For a more quantitative analysis of apoptosis, a well established sensor system, as described e.g. in [21,22] appears to be useful, and morphological studies, e.g. by scattering microscopy with angular or spectral resolution [23], may provide further information.

In a further step towards clinical application, cell monolayers may be replaced by 3-dimensional cell cultures, whose physiology, morphology and nutrient supply is closer to the *in vivo* situation in tumors [24]. Methods of 3D microscopy, e.g., laser scanning microscopy [25,26], structured illumination microscopy [27,28] or light sheet microscopy [29,30] are available for those investigations, and microfluidic systems (see e.g., [31]) may be used for application of appropriate drug doses.

### 3. Experimental Section

#### 3.1. Materials

MCF-7 human breast cancer cells were obtained from Cell Lines Service (CLS No. 00273, Eppelheim, Germany). Cells were routinely grown in DMEM/HAM F-12 medium supplemented with 10% fetal calf serum and antibiotics at 37 °C and 5% CO<sub>2</sub>. Water soluble methyl-β-cyclodextrine (MBCD) as well as the antitumor antibiotic doxorubicin hydrochloride was obtained from Sigma-Aldrich (München, Germany). Doxorubicin was prepared as a 2 μM stock solution in ethanol. After seeding 200 cells/mm<sup>2</sup>, cells were grown on microscope object slides for 48 h prior to incubation with doxorubicin (2 μM). Part of the cells was first incubated with MBCD (4 mM, 15 min) in culture medium without serum for cholesterol depletion. Subsequently cells were incubated with doxorubicin in culture medium for 2 or 24 h at 37 °C. Cholesterol depletion after application of MBCD is well documented in the literature [18]. For spectroscopic measurements cells were seeded in culture flasks, and incubated with MBCD and doxorubicin as described for the cells on object slides. After doxorubicin incubation cells were detached using trypsin/EDTA. After centrifugation and removing the supernatant, the cell pellet was re-suspended in Earl's Balanced Salt Solution (EBSS).  $1 \times 10^6$  cells in a volume of 1.5 mL EBSS were transferred to a glass cuvette.

#### 3.2. Experimental Setup

A diode laser with high repetition pulses (LDH 470 with driver PDL 800-B, Picoquant, Berlin, Germany; wavelength: 470 nm; pulse energy: 12 pJ, pulse duration: 55 ps, repetition rate: 40 MHz; average power: 0.5 mW) was adapted to a fluorescence microscope (Axioplan 1, Carl Zeiss Jena, Germany) by fibre optics for epi-illumination of whole cells. Fluorescence images were recorded by an electron multiplying (EM-) CCD camera with Peltier cooling and a sensitivity below 10<sup>-16</sup> W/Pixel (DV887DC, ANDOR Technology, Belfast, UK) [32] using a long pass filter for  $\lambda \geq 520$  nm. For fluorescence decay kinetics and lifetime images (FLIM) a time-gated image intensifying camera (Picostar HR 12; LaVision, Göttingen, Germany) with a temporal resolution of 200 ps was used in a sampling mode (time range: 8 ns; exposure time: 1 second per channel). Data were fitted as mono-exponential curves [33], and median values as well as median absolute deviations (MADs) of fluorescence lifetimes were determined. Differences were examined by a non-directional Mann-Whitney *U* test [34] for non-normal distributions of experimental values with a level of significance  $\alpha = 5\%$ . A grating spectrometer (Jobin Yvon, JY.3 447) operated at a spectral resolution of 10 nm was used for recording fluorescence spectra of cell suspensions in a glass cuvette. A commercial program (Unscrambler 9.8; Camo process As, Oslo, Norway) was used for Principal Component Analysis.

### 4. Conclusions

As demonstrated above, a combination of fluorescence spectroscopy, fluorescence imaging and fluorescence decay kinetics may be useful to measure cellular uptake, intracellular distribution and intermolecular interactions of the chemotherapeutic drug doxorubicin in cancer cells prior and during

apoptosis. In particular, uptake of doxorubicin and drug response (assessed by changes in fluorescence lifetime) were examined in the context of cholesterol dependent membrane fluidity. Cholesterol content is suggested to be considered for future application of chemotherapeutic drugs.

### Acknowledgments

Present research was funded by the Land Baden-Württemberg and the European Union, Europäischer Fonds für die regionale Entwicklung. The authors thank W.S.L. Strauss and R. Wittig, ILM Ulm, for stimulating ideas and C. Hintze for skillful technical assistance.

### Conflict of Interest

The authors declare no conflict of interest.

### References

1. Carter, S.K.; Blum, R.H. New chemotherapeutic agents—Bleomycin and adriamycin. *CA Cancer J. Clin.* **1974**, *24*, 322–331.
2. Blum, R.H.; Carter, S.K. Adriamycin. A new anticancer drug with significant clinical activity. *Ann. Intern. Med.* **1974**, *80*, 249–259.
3. Li, Z.X.; Wang, T.T.; Wu, Y.T.; Xu, C.M.; Dong, M.Y.; Sheng, J.Z.; Huang, H.F. Adriamycin induces H2AX phosphorylation in human spermatozoa. *Asian J. Androl.* **2008**, *10*, 749–757.
4. Karukstis, K.K.; Thompson, E.H.; Whiles, J.A.; Rosenfeld, R.J. Deciphering the fluorescence signature of daunomycin and doxorubicin. *Biophys. Chem.* **1998**, *73*, 249–263.
5. Chen, N.T.; Wu, C.Y.; Chung, C.Y.; Hwu, Y.; Cheng, S.H.; Mou, C.Y.; Lo, L.W. Probing the dynamics of doxorubicin-DNA intercalation during the initial activation of apoptosis by fluorescence lifetime imaging microscopy (FLIM). *PLoS One* **2012**, *7*, e44947.
6. Bakker, G.J.; Andresen, V.; Hoffman, R.M.; Friedl, P. Fluorescence lifetime microscopy of tumor cell invasion, drug delivery, and cytotoxicity. *Methods Enzymol.* **2012**, *504*, 109–125.
7. Dai, X.; Yue, Z.; Eccleston, M.E.; Swartling, J.; Slater, N.K.; Kaminski, C.F. Fluorescence intensity and lifetime imaging of free and micellar-encapsulated doxorubicin in living cells. *Nanomedicine* **2008**, *4*, 49–56.
8. Haaland, D.M.; Jones, H.D.; van Benthem, M.H.; Sinclair, M.B.; Melgaard, D.K.; Stork, C.L.; Pedroso, M.C.; Liu, P.; Brasier, A.R.; Andrews, N.L.; *et al.* Hyperspectral confocal fluorescence imaging: Exploring alternative multivariate curve resolution approaches. *Appl. Spectrosc.* **2009**, *63*, 271–279.
9. Schneckenburger, H.; Weber, P.; Wagner, M.; Schickinger, S.; Richter, V.; Bruns, T.; Strauss, W.S.; Wittig, R. Light exposure and cell viability in fluorescence microscopy. *J. Microsc.* **2012**, *245*, 311–318.
10. Slingerland, M.; Guchelaar, H.J.; Gelderblom, H. Liposomal drug formulations in cancer therapy: 15 years along the road. *Drug Discov. Today* **2012**, *17*, 160–166.

11. Opel, D.; Westhoff, M.A.; Bender, A.; Braun, V.; Debatin, K.M.; Fulda, S. Phosphatidylinositol 3-kinase inhibition broadly sensitizes glioblastoma cells to death receptor- and drug-induced apoptosis. *Cancer Res.* **2008**, *68*, 6271–6280.
12. Regev, R.; Eytan, G.D. Flip-flop of doxorubicin across erythrocyte and lipid membranes. *Biochem. Pharmacol.* **1997**, *54*, 1151–1158.
13. Pacilio, C.; Florio, S.; Pagnini, U.; Crispino, A.; Claudio, P.P.; Pacilio, G.; Pagnini, G. Modification of membrane fluidity and depolarization by some anthracyclines in different cell lines. *Anticancer Res.* **1998**, *18*, 4027–4034.
14. Storch, C.H.; Eehalt, R.; Haefeli, W.E.; Weiss, J. Localization of the human breast cancer resistance protein (BCRP/ABCG2) in lipid rafts/caveolae and modulation of its activity by cholesterol *in vitro*. *J. Pharmacol. Exp. Ther.* **2007**, *323*, 257–264.
15. Peetla, C.; Bhave, R.; Vijayaraghavalu, S.; Stine, A.; Kooijman, E.; Labhasetwar, V. Drug resistance in breast cancer cells: Biophysical characterization of and doxorubicin interactions with membrane lipids. *Mol. Pharm.* **2010**, *7*, 2334–2348.
16. Weber, P.; Wagner, M.; Schneckenburger, H. Fluorescence imaging of membrane dynamics in living cells. *J. Biomed. Opt.* **2010**, *15*, 046017.
17. von Arnim, C.A.; von Einem, B.; Weber, P.; Wagner, M.; Schwanzar, D.; Spoelgen, R.; Strauss, W.L.; Schneckenburger, H. Impact of cholesterol level upon APP and BACE proximity and APP cleavage. *Biochem. Biophys. Res. Commun.* **2008**, *370*, 207–212.
18. Christian, A.E.; Haynes, M.P.; Phillips, M.C.; Rothblat, G.H. Use of cyclodextrins for manipulating cellular cholesterol content. *J. Lipid Res.* **1997**, *38*, 2264–2272.
19. Eker, C.; Rydell, R.; Svanberg, K.; Andersson-Engels, S. Multivariate analysis of laryngeal fluorescence spectra recorded *in vivo*. *Lasers Surg. Med.* **2001**, *28*, 259–266.
20. Qu, J.Y.; Chang, H.; Xiong, S. Fluorescence spectral imaging for characterization of tissue based on multivariate statistical analysis. *J. Opt. Soc. Am. A* **2002**, *19*, 1823–1831.
21. Xu, X.; Gerard, A.L.; Huang, B.C.; Anderson, D.C.; Payan, D.G.; Luo, Y. Detection of programmed cell death using fluorescence energy transfer. *Nucleic Acids Res.* **1998**, *26*, 2034–2035.
22. Angres, B.; Steuer, H.; Weber, P.; Wagner, M.; Schneckenburger, H. A membrane-bound FRET-based caspase sensor for detection of apoptosis using fluorescence lifetime and total internal reflection microscopy. *Cytometry A* **2009**, *75*, 420–427.
23. Mulvey, C.S.; Sherwood, C.A.; Bigio, I.J. Wavelength-dependent backscattering measurements for quantitative real-time monitoring of apoptosis in living cells. *J. Biomed. Opt.* **2009**, *14*, 064013.
24. Kunz-Schughart, L.A.; Freyer, J.P.; Hofstaedter, F.; Ebner, R. The use of 3-D cultures for high-throughput screening: The multicellular spheroid model. *J. Biomol. Screen* **2004**, *9*, 273–285.
25. Pawley, J. *Handbook of Biological Confocal Microscopy*; Plenum Press: New York, NY, USA, 1990.
26. Webb, R.H. Confocal optical microscopy. *Rep. Prog. Phys.* **1996**, *59*, 427–471.
27. Neil, M.A.; Juskaitis, R.; Wilson, T. Method of obtaining optical sectioning by using structured light in a conventional microscope. *Opt. Lett.* **1997**, *22*, 1905–1907.

28. Gustafsson, M.G.; Shao, L.; Carlton, P.M.; Wang, C.J.; Golubovskaya, I.N.; Cande, W.Z.; Agard, D.A.; Sedat, J.W. Three-dimensional resolution doubling in wide-field fluorescence microscopy by structured illumination. *Biophys. J.* **2008**, *94*, 4957–4970.
29. Huisken, J.; Swoger, J.; Del Bene, F.; Wittbrodt, J.; Stelzer, E.H. Optical sectioning deep inside live embryos by selective plane illumination microscopy. *Science* **2004**, *305*, 1007–1009.
30. Santi, P.A. Light sheet fluorescence microscopy: A review. *J. Histochem. Cytochem.* **2011**, *59*, 129–138.
31. Bruns, T.; Schickinger, S.; Wittig, R.; Schneckenburger, H. Preparation strategy and illumination of three-dimensional cell cultures in light sheet-based fluorescence microscopy. *J. Biomed. Opt.* **2012**, *17*, 101518.
32. Coates, C.G.; Denvir, D.J.; McHale, N.G.; Thornbury, K.D.; Hollywood, M.A. Optimizing low-light microscopy with back-illuminated electron multiplying charge-coupled device: Enhanced sensitivity, speed, and resolution. *J. Biomed. Opt.* **2004**, *9*, 1244–1252.
33. Schneckenburger, H.; Wagner, M.; Kretzschmar, M.; Strauss, W.S.; Sailer, R. Laser-assisted fluorescence microscopy for measuring cell membrane dynamics. *Photochem. Photobiol. Sci.* **2004**, *3*, 817–822.
34. Wilcoxon, F. Individual comparisons by ranking methods. *Biometrics Bull.* **1945**, *1*, 80–83.

© 2013 by the authors; licensee MDPI, Basel, Switzerland. This article is an open access article distributed under the terms and conditions of the Creative Commons Attribution license (<http://creativecommons.org/licenses/by/3.0/>).